Stem Cell Reports
Report
OPEN ACCESS

Efficient Generation of Myelinating Oligodendrocytes from Primary Progressive Multiple Sclerosis Patients by Induced Pluripotent Stem Cells

Panagiotis Douvaras,[1] Jing Wang,[2] Matthew Zimmer,[1] Stephanie Hanchuk,[1] Melanie A. O'Bara,[2] Saud Sadiq,[3] Fraser J. Sim,[2] James Goldman,[4] and Valentina Fossati[1,*]
[1]The New York Stem Cell Foundation Research Institute, New York, NY 10032, USA
[2]Department of Pharmacology and Toxicology, School of Medicine and Biomedical Sciences, University at Buffalo, Buffalo, NY 14214, USA
[3]Tisch Multiple Sclerosis Research Center of New York, New York, NY 10019, USA
[4]Department of Pathology and Cell Biology, Columbia University, New York, NY 10032, USA
*Correspondence: vfossati@nyscf.org
http://dx.doi.org/10.1016/j.stemcr.2014.06.012

SUMMARY

Multiple sclerosis (MS) is a chronic demyelinating disease of unknown etiology that affects the CNS. While current therapies are primarily directed against the immune system, the new challenge is to address progressive MS with remyelinating and neuroprotective strategies. Here, we develop a highly reproducible protocol to efficiently derive oligodendrocyte progenitor cells (OPCs) and mature oligodendrocytes from induced pluripotent stem cells (iPSCs). Key elements of our protocol include adherent cultures, dual SMAD inhibition, and addition of retinoids from the beginning of differentiation, which lead to increased yields of OLIG2 progenitors and high numbers of OPCs within 75 days. Furthermore, we show the generation of viral and integration-free iPSCs from primary progressive MS (PPMS) patients and their efficient differentiation to oligodendrocytes. PPMS OPCs are functional, as demonstrated by in vivo myelination in the shiverer mouse. These results provide encouraging advances toward the development of autologous cell therapies using iPSCs.

INTRODUCTION

Multiple sclerosis (MS) is a chronic, inflammatory, demyelinating disease of the CNS that is distinguished by recurrent episodes of focal inflammatory demyelination and consequent neurological symptoms (relapsing remitting MS [RRMS]). Although relapses usually resolve in spontaneous remission, RRMS can evolve with time into a secondary progressive form characterized by irreversible accumulation of disabilities. Furthermore, patients affected by the most severe primary progressive form (PPMS) experience a steady neurological decline from the onset of the disease (Antel et al., 2012). Currently available treatments targeting the immune system are highly effective at reducing or even stopping the intermittent episodes of inflammation, but they do not influence the course of progressive MS. Therapeutic options for PPMS patients are limited to symptomatic treatments and the long-term prognosis is generally poor (Rice et al., 2013). Clearly, the unsolved challenge in the MS field is to develop neuroprotective and remyelinating strategies for the treatment of progressive MS patients (Hauser et al., 2013). The generation of patient-specific cells from induced pluripotent stem cells (iPSCs) or somatic cell nuclear transfer has recently emerged as a promising strategy for the development of autologous cell therapies (Goldman et al., 2012; Yamada et al., 2014). iPSC-derived oligodendrocyte progenitor cells (OPCs) were shown to successfully remyelinate and rescue a hypomyelinated mouse model, raising the possibility of future clinical trials (Wang et al., 2013). However, oligodendrocyte differentiation protocols are still inefficient and require over 120 days in culture. Therefore, an improved protocol that can generate large numbers of purified OPCs in a relatively short time is highly desirable. Moreover, this protocol should be reproducible and highly efficient among different iPSC lines, including those derived from MS patients. We have pioneered the efficient and robust generation of iPSC-derived OPCs from PPMS patients. Our protocol recapitulates the major steps of oligodendrocyte differentiation from neural stem cells to $OLIG2^+$ progenitors and finally to $O4^+$ OPCs in a significantly shorter time than the 120–150 days required by the most recently published protocols (Wang et al., 2013; Stacpoole et al., 2013). Furthermore, $O4^+$ OPCs were able to differentiate into MBP^+ mature oligodendrocytes in vitro and to myelinate axons in vivo when injected into immunocompromised shiverer (*shi/shi*) mice. No abnormal growths were observed. Our results provide a proof of concept that transplantation of iPSC-derived, patient-specific cells for remyelination is technically feasible.

RESULTS

Retinoic Acid Is Critical for Efficient Differentiation of PSCs to Oligodendrocytes

We aimed to develop an efficient differentiation protocol that recapitulates the critical developmental stages of oligodendrocyte specification as it occurs in the spinal cord. In this process, $PAX6^+$ neural stem cells give rise to $OLIG2^+$

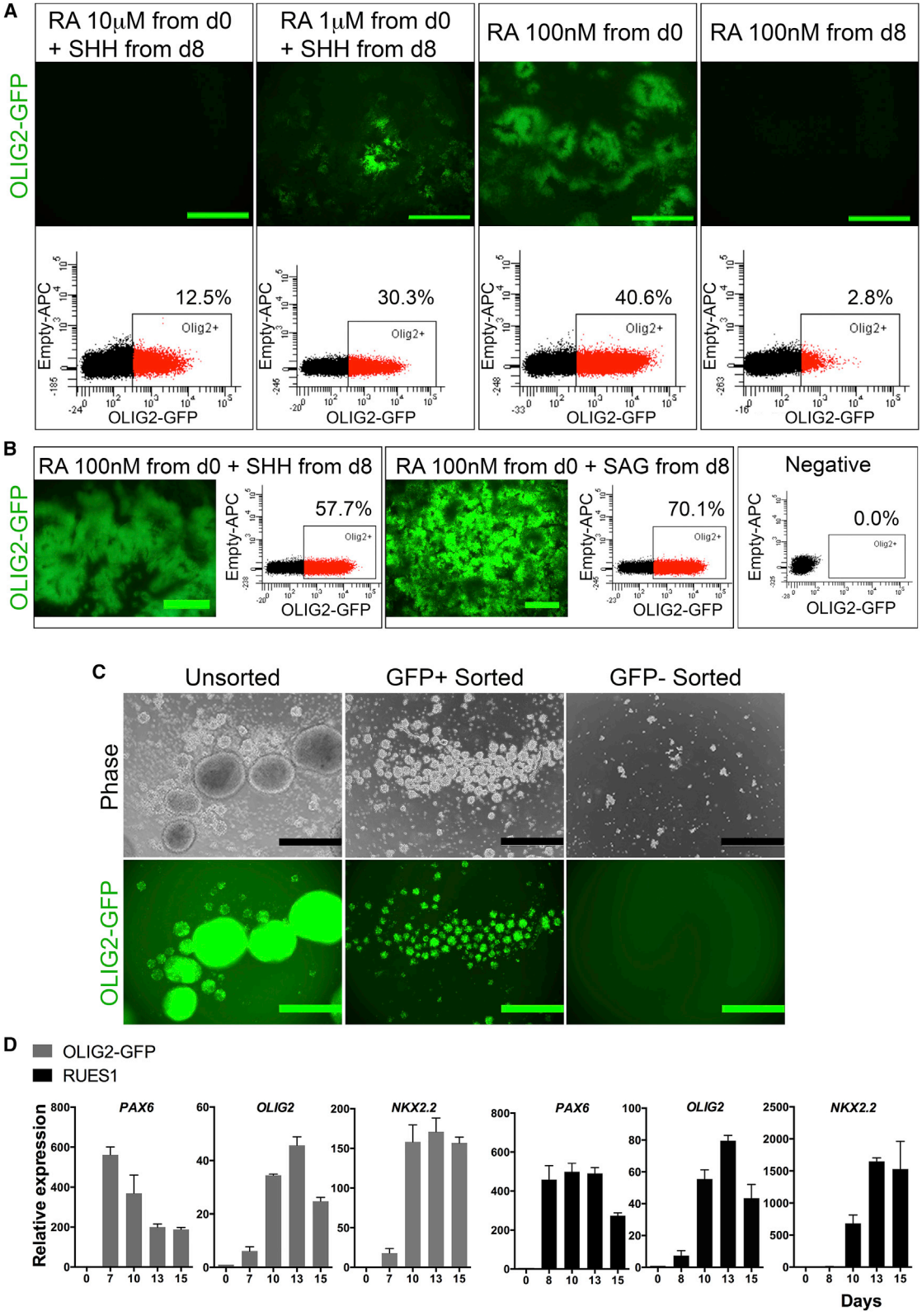

(legend on next page)

progenitors, which become committed to the oligodendrocyte lineage by coexpressing NKX2.2 (pre-OPCs). They then differentiate to early OPCs by upregulating SOX10 and PDGFRα, followed by late OPCs expressing the sulfated glycolipid antigen recognized by the O4 antibody, and finally mature to myelin basic protein (MBP)$^+$ oligodendrocytes (Hu et al., 2009a). We utilized an OLIG2-GFP knockin human embryonic stem cell (hESC) reporter line to track the OLIG2$^+$ progenitors by live fluorescent imaging (Liu et al., 2011). First, we induced PAX6$^+$ cells using dual inhibition of SMAD signaling in adherent cultures (Chambers et al., 2009). Next, to mimic the embryonic spinal cord environment, we applied different concentrations of retinoic acid (RA) and/or sonic hedgehog (SHH) at various times and quantified the OLIG2-GFP expression by flow cytometry (Figure 1A). Application of 100 nM RA from the beginning of induction generated 40.6% of OLIG2$^+$ progenitors, whereas addition of SHH at 100 ng/ml from day 8 increased the yield to 57.7% (Figure 1B). Interestingly, cells without exogenous SHH during the first 12 days showed an upregulation of *SHH* mRNA (Figure S1A available online) and differentiated to O4$^+$ cells, although at a lower efficiency compared with cells treated with SHH (Figure S1B). We then replaced the recombinant human SHH protein with the smoothened agonist (SAG), which increased the yield further to 70.1% OLIG2$^+$ progenitors (Figure 1B). At day 12, cells were detached for sphere aggregation. The minimum number of cells required to form a sphere was 100, and we noted that the majority of the cells in the spheres were GFP$^+$. To investigate this further, we sorted d12 cultures for GFP and observed that only GFP$^+$ cells formed aggregates, whereas the GFP$^-$ population did not (Figure 1C). This suggests that the aggregation step alone provides enrichment for the OLIG2$^+$ population.

Next, we validated the initial steps toward the generation of OLIG2$^+$ progenitors by differentiating a second hESC line (RUES1) and comparing the transcript levels of *PAX6*, *OLIG2*, and *NKX2.2* by quantitative RT-PCR (qRT-PCR). The upregulation of these transcription factors followed a temporal pattern similar to that of the OLIG2-GFP line, with *PAX6* induction around day7, *OLIG2* peak around day 13, and sustainably high levels of *NKX2.2* after day 10 (Figure 1D). Based on these results, we used the nongenetically modified RUES1 line to develop the following steps of the protocol from OLIG2$^+$ progenitors to MBP$^+$ mature oligodendrocytes (Figure 2A). PAX6$^+$ cells arose at day 7, and by day 12 they were arranged into multilayered structures (Figures 2B and 2C). From day 12 to day 30 the cells were grown as spheres, and they were then plated onto poly-L-ornithine/laminin-coated dishes for the remainder of the differentiation protocol.

To promote maturation toward the O4$^+$ stage, platelet-derived growth factor AA (PDGF-AA), hepatocyte growth factor (HGF), insulin-like growth factor 1 (IGF1), and neurotrophin 3 (NT3) were added to the culture medium from day 20 onward. OLIG2$^+$ progenitors upregulated NKX2.2 (pre-OPCs) and then SOX10 (early OPCs), and they finally matured to late OPCs, which were identified by O4 live staining and by their highly ramified processes (Figures 2D–2G). O4$^+$ OPCs expressing OLIG2, SOX10, and NG2 (Figures 2H–2J) appeared as early as day 50 and increased dramatically around day 75. During the differentiation, 40%–50% of progenitor cells were proliferative, as indicated by Ki67 staining. However, the highly ramified O4$^+$ cells did not divide in vitro (Figures S2A–S2C). Additionally, 34% ± 4% of O4$^+$ OPCs differentiated into MBP$^+$ mature oligodendrocytes after growth-factor withdrawal from the medium for at least 3 weeks (Figures 2K, 2L, and S2D). Our cultures also consisted of other cell types (15% ± 2% GFAP$^+$ astrocytes and 20% ± 2% MAP2$^+$ neurons of total cells, respectively; Figures 2M and S2E).

Oligodendrocytes Can Be Efficiently Generated from PPMS-iPSC Lines

To determine whether this protocol could be applied to iPSC lines from subjects with PPMS, we obtained skin biopsies from four PPMS patients. Fibroblast cultures were established from the biopsies and iPSCs were generated using a cocktail of modified mRNAs (Warren et al., 2010) together with a cluster of miRNAs to improve the reprogramming efficiency (StemGent). From day 12 to day 15 of reprogramming, TRA-1-60$^+$ colonies (Figure S3A), identified by live staining, were picked, expanded, and characterized by immunofluorescence for pluripotency markers (Figure S3B).

Figure 1. RA and SHH Requirement to Derive OLIG2$^+$ Progenitor Cells

(A) Live imaging and flow-cytometric quantification of OLIG2-GFP cells at day 14 of differentiation under different conditions for RA and SHH.

(B) Comparison between the addition of SHH or SAG at day 8 and the best RA condition via live imaging and FACS analysis. Negative: hESC line RUES1.

(C) Assessment of sphere formation for unsorted or sorted GFP$^+$ and GFP$^-$ cells.

(D) Temporal gene-expression profile for *PAX6*, *OLIG2*, and *NKX2.2* under optimal RA and SHH conditions. Error bars are SEM (n = 3 independent experiments). Scale bars represent 500 μm.

See Figure S1 for further optimizations of RA and SHH.

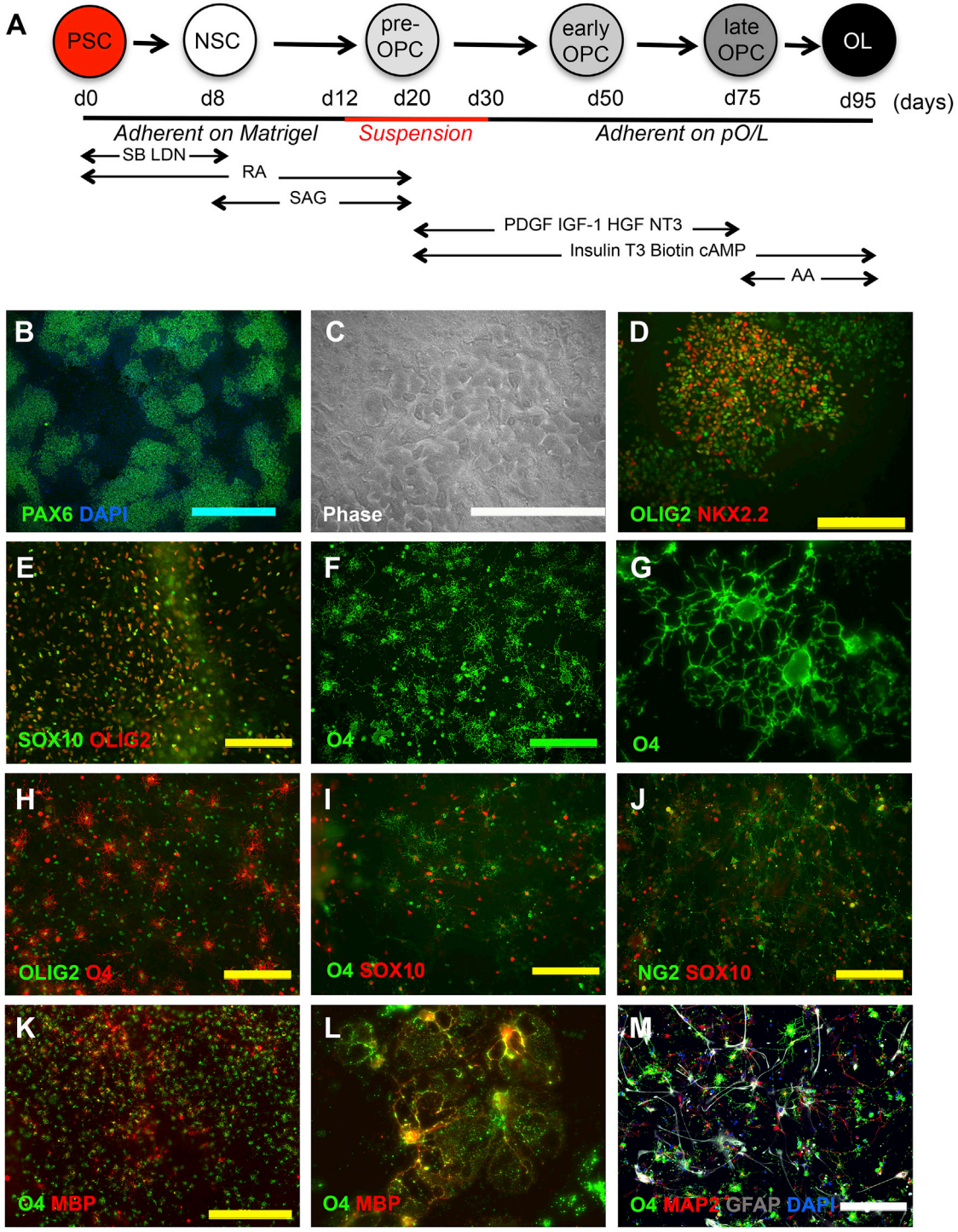

Figure 2. Generation of Oligodendrocytes from Human PSCs

(A) Diagram of the protocol for differentiation from hPSCs to mature oligodendrocytes.

(B–M) Sequential steps of in vitro oligodendrocyte differentiation of RUES1 cells, showing PAX6$^+$ neural stem cells at day 8 (B), phase contrast of the multilayered structures at day 12 (C), OLIG2$^+$NKX2.2$^+$ pre-OPCs at day 18 (D), SOX10$^+$OLIG2$^+$ early OPCs (E), live imaging of O4$^+$ late OPCs (F), a cropped image of O4$^+$ cells to highlight the ramified processes (G), O4$^+$ OPCs coexpressing OLIG2 (H), O4$^+$ OPCs coexpressing SOX10 (I), sorted O4$^+$ OPCs coexpressing SOX10 and NG2 (J), terminally differentiated MBP$^+$ oligodendrocytes at low (K) and

(legend continued on next page)

Expression profiling for seven pluripotency genes confirmed that all four iPSC lines exhibited a profile comparable to that of a reference hESC line and divergent from the parental fibroblasts (Figure S3C). All iPSC lines displayed a normal karyotype (Figure S3D) and were able to differentiate into cell types of the three germ layers, both in vitro via spontaneous embryoid body differentiation (Figure S3E) and in vivo via teratoma assay (Figure S3F).

Next, we assessed whether the oligodendrocyte differentiation protocol was reproducible with our PPMS-iPSC lines. All iPSC lines tested were found to perform similarly to the RUES1 line (Figures 3A–3I). The protocol was greatly reproducible and highly efficient as calculated by the frequency of sorted $O4^+$ OPCs, with up to 70% $O4^+$ cells from RUES1 and 43.6%–62.1% from the PPMS-iPSC lines. Additionally, we found that the $O4^+$ fraction contained a subpopulation of cells double positive with PDGFRα (Figure 3J). $O4^+$ cells could be easily purified by fluorescence-activated cell sorting (FACS), frozen, and thawed without losing their morphology (Figure S4D).

PPMS-Derived Late OPCs Myelinate Axons in the Mouse Brain

To verify that OPCs obtained through our protocol were functionally myelinogenic, we injected d75 FACS-purified $O4^+$ cells into the forebrain of neonatal, immunocompromised shiverer mice (10^5 cells/animal; Figure S4A). The injected cells were depleted of any contaminant iPSCs, as shown by flow-cytometry analysis of the pluripotency markers SSEA4 and TRA-1-60 (Figure S4B). However, we still purified our cultures before in vivo transplantation to retain the potential for translation to clinical studies. Cells were frozen, thawed, and allowed to recover for 24–48 hr before transplantation (Figure S4C). Animals were sacrificed at 12–16 weeks, at which point human hNA^+ cells were distributed throughout the corpus callosum and forebrain white matter. The density of hNA^+ cells in the corpus callosum was 34,400 ± 3,090 cells/mm^3 at 12 weeks and approximately double that by 16 weeks. We did not observe the presence of cell clusters or overt tumorigenesis, and the proliferative fraction of engrafted hNA^+ cells was 17% at 12 weeks and decreased to only 8% $Ki67^+$ at 16 weeks when only 5% of cells were $PCNA^+$ (Figure 4H). Importantly, more than 80% of hNA^+ cells in the corpus callosum coexpressed OLIG2 protein, suggesting that the engrafted cells were restricted to the oligodendrocyte lineage (Figure 4I). Furthermore, human MBP^+ oligodendrocytes were found diffusely throughout engrafted corpus callosum at 12 and 16 weeks (Figure 4A). At 16 weeks, 31% ± 3% of host mouse axons were ensheathed within the engrafted mouse corpus callosum (Figure 4B).

We then asked whether PPMS-derived OPCs could form compact myelin. Transmission electron microscopy on 16-week-old corpus callosum revealed mature compact myelin with the presence of alternating major dense and intraperiod lines (Figures 4C and 4D), whereas uninjected shiverer/*rag2* mice possessed thin and loosely wrapped myelin (data not shown). Likewise, the thickness of myelin ensheathment, as assessed by g-ratio measurement, reflected a restoration of normal myelin in several callosal axons.

At 12 weeks, transplanted cells remained as $NG2^+$ OPCs in the corpus callosum (Figure 4E), and by 16 weeks they started to migrate to the overlying cerebral cortex (Figure 4F). Very few O4-sorted cells underwent differentiation as $hGFAP^+$ astrocytes and the majority of $hGFAP^+$ cells were localized to the subventricular zone and around the ventricles (Figure 4G), suggesting that the local environment may induce astrocytic differentiation in these regions. Similarly, hNESTIN-expressing cells were rarely found in the corpus callosum and likewise concentrated in the subventricular zone (data not shown). Importantly, βIII-$TUBULIN^+$ neurons were not detected in any of the engrafted animals. Taken together, our data demonstrate that PPMS-derived, O4-sorted cells were capable of achieving mature oligodendrocyte differentiation in vivo and forming dense compact myelin resembling normal myelin in the brain.

DISCUSSION

In this work, using a fast and highly reproducible protocol, we demonstrated efficient in vivo myelination of neurons by iPSC-derived OPCs from PPMS patients. A previous report on MS-derived iPSCs showed that oligodendrocytes could be differentiated in vitro from an integrating, retrovirally reprogrammed iPSC line from one 35-year-old RRMS patient (Song et al., 2012); here, we generated four integration-free iPSC lines from PPMS patients of both sexes and with ages ranging from 50 to 62 years.

Since most protocols for oligodendrocyte differentiation have been optimized using only one or two hESC lines and their reproducibility with iPSC lines is controversial (Alsanie et al., 2013), we tested our protocol with two hESC and four hiPSC lines derived from PPMS patients. Previous

higher (×64; L) magnification, and $MAP2^+$ and $GFAP^+$ cells in oligodendrocyte cultures (M). PSC, pluripotent stem cell; NSC, neural stem cell; OPC, oligodendrocyte progenitor cell; OL, oligodendrocyte; pO/L, poly-L-ornithine/laminin.
Scale bars represent 500 μm (B and K), 2 mm (C), and 200 μm (D–F, H–J, and M). See also Figure S2 for proliferation assessment and quantification of MBP^+ OLs and $MAP2^+$ and $GFAP^+$ cells.

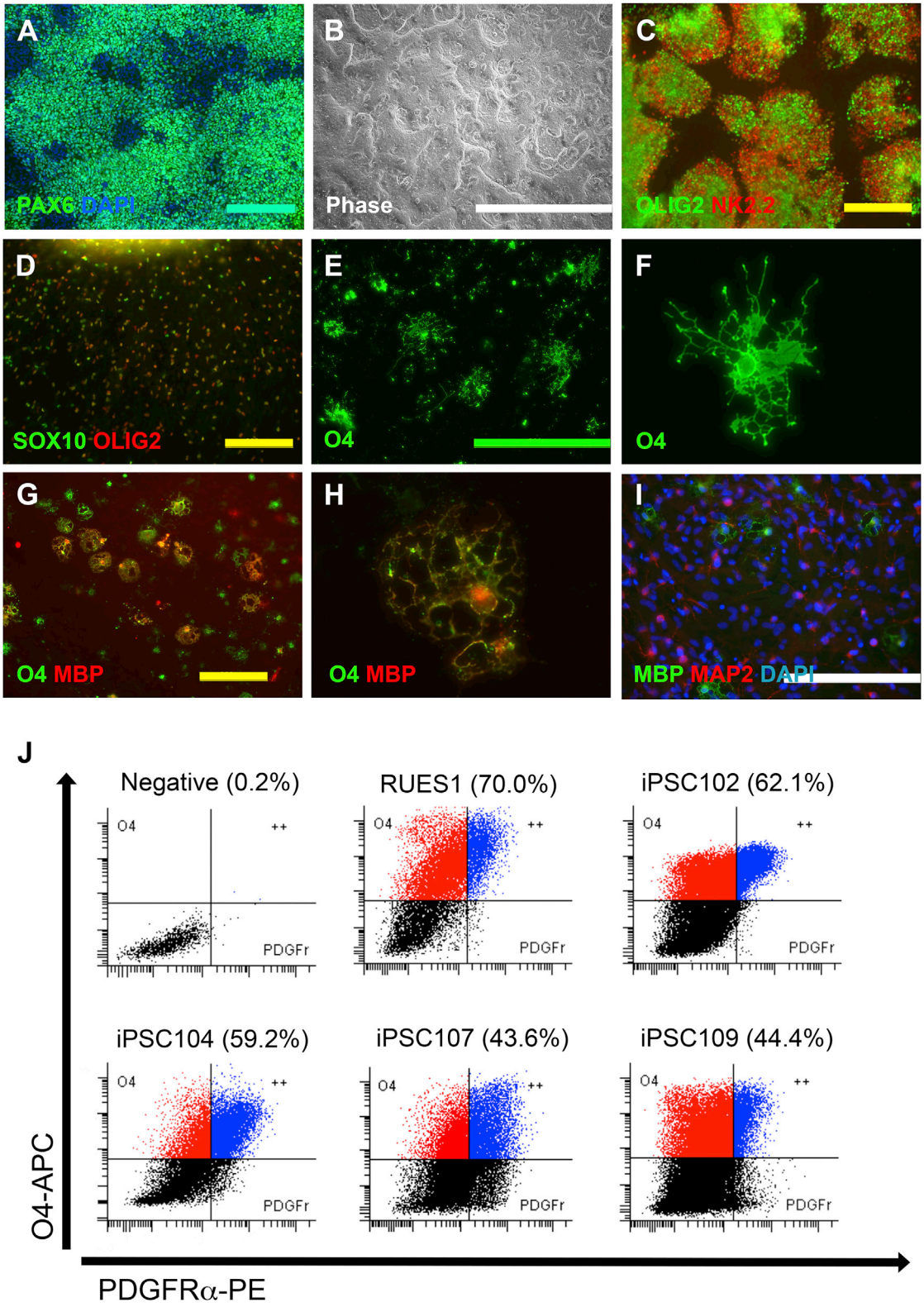

Figure 3. PPMS iPSCs Generate OPCs and Mature Oligodendrocytes In Vitro

(A–I) Sequential steps of in vitro oligodendrocyte differentiation of PPMS iPSCs, showing PAX6$^+$ cells at day 8 (A), multilayered structures in phase contrast at day 12 (B), OLIG2$^+$ and NKX2.2$^+$ cells at day 12 (C), SOX10$^+$OLIG2$^+$ early OPCs (D), live imaging of O4$^+$ late OPCs at day

(legend continued on next page)

work has elegantly shown that iPSC-derived OPCs from healthy controls were able to rescue a mouse model of hypomyelination, although differentiation to the O4 stage was rather inefficient and required more than 120 days (Wang et al., 2013). We provide an improved differentiation protocol and further proof that patient-specific iPSC lines can be successfully used to generate oligodendrocytes. We obtained 44%–70% $O4^+$ cells in all lines after 75 days of differentiation, compared with the minimum of 120 days required according to previous reports (Wang et al., 2013; Stacpoole et al., 2013). There are several critical differences between our approach and previously published protocols. First, we began neural induction with dual SMAD inhibition in adherent as opposed to suspension cultures (Nistor et al., 2005; Hu et al., 2009b; Wang et al., 2013). Using this approach, we started with only 10,000 cells/cm^2 of iPSCs at day 0 and achieved a great expansion of neural progenitors, ultimately generating an abundance of human OPCs. The use of RA and SHH as caudalizing and ventralizing patterning agents recapitulates the signals that are present around the pMN domain of the spinal cord, from which motor neurons and oligodendrocytes are believed to arise (Hu et al., 2009a). The high efficiency in the generation of $OLIG2^+$ cells at d12 can be explained by the synergistic effect of activin/nodal receptor kinase inhibition, BMP4 inhibition, and RA and SHH signaling (Patani et al., 2011; Miller et al., 2004). The optimal concentration of RA in our hands is 100 times less than the concentration commonly used by other groups (Nistor et al., 2005; Izrael et al., 2007; Gil et al., 2009; Hu et al., 2009b). Surprisingly, induction with RA alone (without exogenous SHH) generated a large population of $OLIG2^+$ cells. While the combination of RA and fibroblast growth factor (FGF) signaling is known to promote OLIG2 expression during chicken development and has been used for in vitro differentiation of both hESCs and hiPSCs (Novitch et al., 2003; Nistor et al., 2005; Pouya et al., 2011), we achieved OLIG2 induction in the absence of any exogenous FGF in our culture conditions. We show that RA, synergistically with the dual inhibition of SMAD proteins, upregulates OLIG2 (Figure S1C), possibly by stimulating the endogenous expression of *SHH* (Figure S1A). We confirmed that SAG is an efficient replacement for SHH and indeed showed superior efficacy in our hands (Stacpoole et al., 2013). The addition of HGF to the medium, although not essential, appeared to slightly improve the differentiation efficiency (data not shown; Hu et al., 2009c). Finally, the transition from adherent cultures to spheres proved to be a critical step to enrich the $OLIG2^+$ population and possibly restrict differentiation to the oligodendrocyte lineage.

In human development, OPCs are characterized by PDGFRα and NG2 expression, followed by expression of O4 (Jakovcevski et al., 2009). Under our culture conditions, by day 75, most of the $O4^+$ cells had lost PDGFRα, but retained NG2 expression. At this stage, we did not observe any residual pluripotent cells in culture. Our study differs from recent work in that our iPSC lines were derived from PPMS patients and the cells used for in vivo transplantation were sorted using the late-OPC marker O4 to maximally restrict the differentiation potential. Despite these differences, the PPMS-derived, $O4^+$-sorted OPCs exhibited a similar engraftment efficiency, mitotic fraction, and proportion of host ensheathed axons while generating fewer $GFAP^+$ astrocytes compared with the unsorted iPSC-derived OPCs reported previously. Taken together, our data suggest that PPMS-derived OPCs performed in vivo at least as efficiently as healthy iPSC-derived cells (Wang et al., 2013).

These proof-of-principle experiments establish that our OPC induction protocol can generate myelinogenic oligodendrocytes from patient samples and may be useful for the development of autologous cell-replacement therapies for MS in the future.

iPSC technology is also emerging as a tool for developing new drugs and gaining insight into disease pathogenesis (Han et al., 2011). Our differentiation protocol will aid the development of high-throughput in vitro screens for compounds that promote myelination (Lee et al., 2013). Furthermore, the PPMS iPSC lines described here provide an additional resource for investigating the process of neurodegeneration in MS. Future studies comparing PPMS iPSCs and appropriate healthy control iPSC lines will be needed to shed light on the potential intrinsic differences among patient-derived oligodendrocytes.

EXPERIMENTAL PROCEDURES

Subjects

Skin biopsies were obtained from deidentified PPMS patients at the Tisch Multiple Sclerosis Research Center of New York, upon institutional review board approval (BRANY) and receipt of informed consent. All four patients were diagnosed with PPMS according to the standard diagnostic criteria. All patients were Caucasian.

73 (E), a cropped image of $O4^+$ cells to highlight the ramified processes (F), MBP^+ mature oligodendrocytes at low (G) and higher (×64; H) magnification, and $MAP2^+$ cells in the oligodendrocyte cultures (I).
(J) Quantification of $O4^+$ cells after 75 days of differentiation from RUES1 and PPMS iPSCs via FACS analysis. Gates are based on secondary Ab-APC only for O4 staining and PE-conjugated isotype control for PDGFRα staining (negative). Total $O4^+$ cells (including O4 single-positive and O4/PDGFRα double-positive cells) are shown in brackets.
Scale bars represent 200 μm (A, C–E, G, and I) and 2 mm (B). See Figure S3 for characterization of PPMS-iPSC lines.

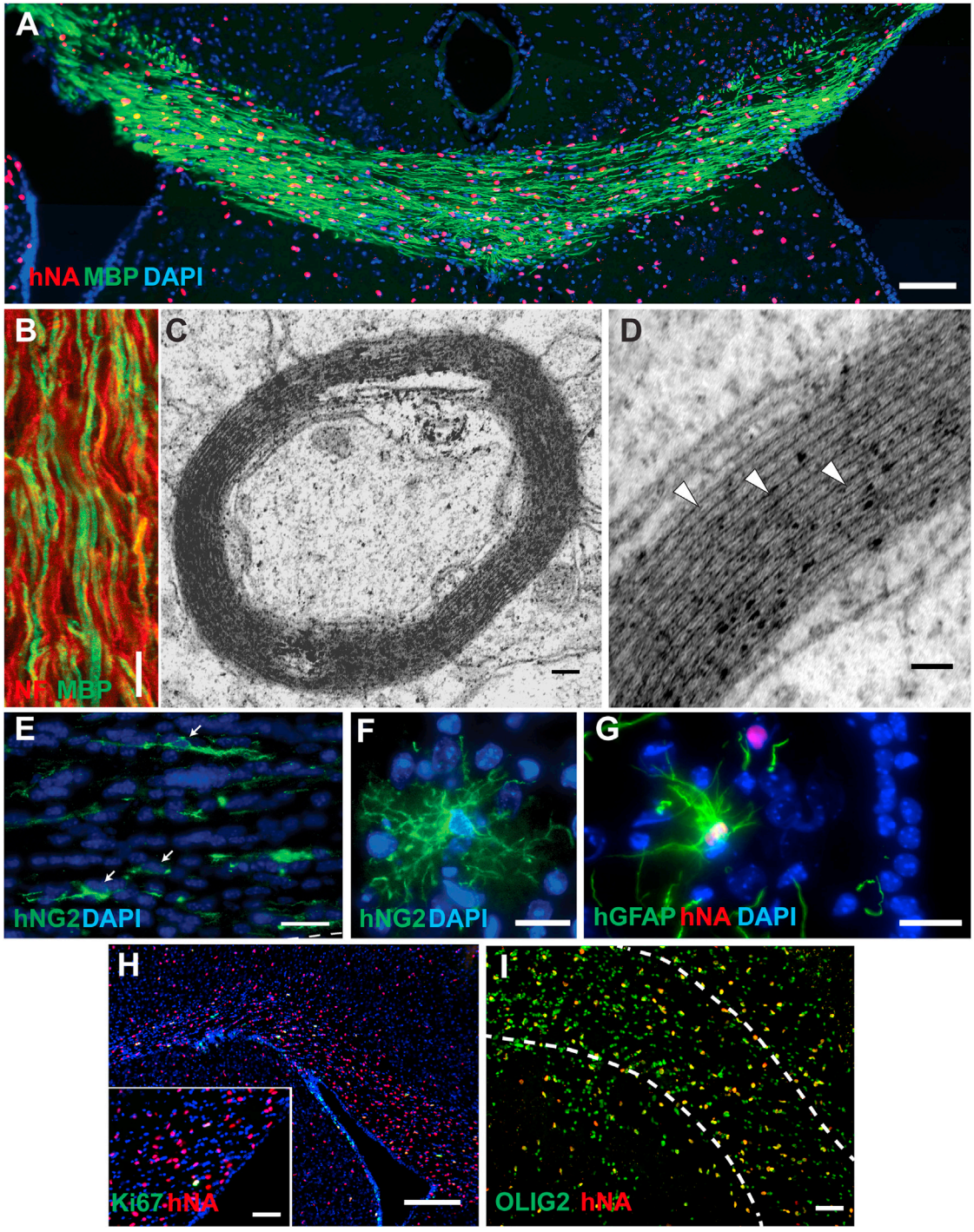

Figure 4. PPMS-Derived OPCs Engraft and Differentiate to Myelinogenic Oligodendrocytes In Vivo

(A) PPMS-iPSC-derived O4$^+$ OPCs (10^5) were transplanted into neonatal shiverer/*rag2* mice. At 16 weeks, MBP$^+$ oligodendrocytes are widely distributed throughout the corpus callosum.

(B) Confocal image showing colocalization of mouse axons and MBP$^+$ human oligodendrocytes.

(C and D) Electron micrographs of myelinated axons exhibiting characteristic compact myelin with alternating major dense (arrowheads) and intraperiod lines.

(E) Human cells retain progenitor characteristics, expressing a human specific-NG2 antigen (individual cells marked by arrows; 12 weeks).

(F) At 16 weeks, individual NG2 cells have begun to migrate into the overlying cerebral cortex.

(legend continued on next page)

Two patients were male (56 and 61 years old) and two were female (62 and 50 years old).

Cell Lines

Three hESC lines and four hiPSC lines were used for the study. RUES1 and HUES 45 are both NIH-approved hESC lines. The OLIG2-GFP reporter line is derived from the BG01 hESC line and was a gift from Dr. Ying Liu (University of Texas Health Science Center at Houston). Four iPSC lines were derived in our laboratory from skin biopsies of PPMS patients through the mRNA/miRNA method (StemGent).

Oligodendrocyte Differentiation Protocol

hESCs and hiPSCs were induced to neural differentiation through dual SMAD inhibition together with 100 nM all-*trans* RA. At day 8, SAG (1 μM) was added to the medium, and at day 12, adherent cells were lifted and seeded in low-attachment plates to favor sphere aggregation. Spheres were cultured in the presence of RA and SAG. At day 30, spheres were plated into poly-L-ornithine/laminin-coated dishes and cells were allowed to migrate out of the sphere. At this stage, PDGF medium was used to promote OPC formation, and from day 75 onward, glial medium was used to drive oligodendrocyte maturation. For the qRT-PCR primer sequences and media compositions used, see Tables S1 and S2, respectively.

Transplantation into Shiverer × *Rag2*$^{-/-}$ Mice

All experiments using shiverer/*rag2* mice (a gift from Dr. Steven A. Goldman, University of Rochester; Windrem et al., 2008) were performed according to protocols approved by the University at Buffalo Institutional Animal Care and Use Committee. Injections were performed as previously described (Sim et al., 2011) and the animals were sacrificed 12–16 weeks later. Cryopreserved coronal sections were cut and immunohistochemistry was performed as described previously (Sim et al., 2011). For transmission electron microscopy, tissue was processed as described previously (Sim et al., 2002). For a list of the primary antibodies used, see Table S3.

SUPPLEMENTAL INFORMATION

Supplemental Information includes Supplemental Experimental Procedures, four figures, and three tables and can be found with this article online at http://dx.doi.org/10.1016/j.stemcr.2014.06.012.

ACKNOWLEDGMENTS

We thank Drs. Dieter Egli and Haiqing Hua for the teratoma study and Dr. Ana Sevilla and Chris Woodard for the nanostring analysis. This work was supported by an NYSCF-Helmsley Early Career Investigator Award, The New York Stem Cell Foundation, and The Leona M. and Harry B. Helmsley Charitable Trust. In vivo studies were supported by the Empire State Stem Cell Fund through the New York State Department of Health (contract C028108 to F.J.S.).

Received: January 6, 2014
Revised: June 23, 2014
Accepted: June 24, 2014
Published: July 24, 2014

REFERENCES

Alsanie, W.F., Niclis, J.C., and Petratos, S. (2013). Human embryonic stem cell-derived oligodendrocytes: protocols and perspectives. Stem Cells Dev. *22*, 2459–2476.

Antel, J., Antel, S., Caramanos, Z., Arnold, D.L., and Kuhlmann, T. (2012). Primary progressive multiple sclerosis: part of the MS disease spectrum or separate disease entity? Acta Neuropathol. *123*, 627–638.

Chambers, S.M., Fasano, C.A., Papapetrou, E.P., Tomishima, M., Sadelain, M., and Studer, L. (2009). Highly efficient neural conversion of human ES and iPS cells by dual inhibition of SMAD signaling. Nat. Biotechnol. *27*, 275–280.

Gil, J.E., Woo, D.H., Shim, J.H., Kim, S.E., You, H.J., Park, S.H., Paek, S.H., Kim, S.K., and Kim, J.H. (2009). Vitronectin promotes oligodendrocyte differentiation during neurogenesis of human embryonic stem cells. FEBS Lett. *583*, 561–567.

Goldman, S.A., Nedergaard, M., and Windrem, M.S. (2012). Glial progenitor cell-based treatment and modeling of neurological disease. Science *338*, 491–495.

Han, S.S.W., Williams, L.A., and Eggan, K.C. (2011). Constructing and deconstructing stem cell models of neurological disease. Neuron *70*, 626–644.

Hauser, S.L., Chan, J.R., and Oksenberg, J.R. (2013). Multiple sclerosis: Prospects and promise. Ann. Neurol. *74*, 317–327.

Hu, B.Y., Du, Z.W., Li, X.J., Ayala, M., and Zhang, S.C. (2009a). Human oligodendrocytes from embryonic stem cells: conserved SHH signaling networks and divergent FGF effects. Development *136*, 1443–1452.

Hu, B.Y., Du, Z.W., and Zhang, S.C. (2009b). Differentiation of human oligodendrocytes from pluripotent stem cells. Nat. Protoc. *4*, 1614–1622.

Hu, Z., Li, T., Zhang, X., and Chen, Y. (2009c). Hepatocyte growth factor enhances the generation of high-purity oligodendrocytes from human embryonic stem cells. Differentiation *78*, 177–184.

Izrael, M., Zhang, P., Kaufman, R., Shinder, V., Ella, R., Amit, M., Itskovitz-Eldor, J., Chebath, J., and Revel, M. (2007). Human oligodendrocytes derived from embryonic stem cells: effect of noggin on phenotypic differentiation *in vitro* and on myelination *in vivo*. Mol. Cell. Neurosci. *34*, 310–323.

(G) Only a few hGFAP$^+$ astrocytes are found in proximity to the lateral ventricle.
(H) Very few of the engrafted human cells are still proliferative 16 weeks after transplantation. Insert is a higher-magnification image.
(I) OLIG2$^+$/hNA$^+$ progenitor cells 16 weeks after transplantation. hNA, human nuclear antigen; NF, neurofilament.
Scale bars represent 100 μm (A), 10 μm (B), 100 nm (C), 50 nm (D), 25 μm (E–G), 200 μm (H and I), and 50 μm (inset in H). See also Figure S4 for details on cells immediately before transplantation.

Jakovcevski, I., Filipovic, R., Mo, Z., Rakic, S., and Zecevic, N. (2009). Oligodendrocyte development and the onset of myelination in the human fetal brain. Front Neuroanat *3*, 5.

Lee, S., Chong, S.Y., Tuck, S.J., Corey, J.M., and Chan, J.R. (2013). A rapid and reproducible assay for modeling myelination by oligodendrocytes using engineered nanofibers. Nat. Protoc. *8*, 771–782.

Liu, Y., Jiang, P., and Deng, W. (2011). OLIG gene targeting in human pluripotent stem cells for motor neuron and oligodendrocyte differentiation. Nat. Protoc. *6*, 640–655.

Miller, R.H., Dinsio, K., Wang, R., Geertman, R., Maier, C.E., and Hall, A.K. (2004). Patterning of spinal cord oligodendrocyte development by dorsally derived BMP4. J. Neurosci. Res. *76*, 9–19.

Nistor, G.I., Totoiu, M.O., Haque, N., Carpenter, M.K., and Keirstead, H.S. (2005). Human embryonic stem cells differentiate into oligodendrocytes in high purity and myelinate after spinal cord transplantation. Glia *49*, 385–396.

Novitch, B.G., Wichterle, H., Jessell, T.M., and Sockanathan, S. (2003). A requirement for retinoic acid-mediated transcriptional activation in ventral neural patterning and motor neuron specification. Neuron *40*, 81–95.

Patani, R., Hollins, A.J., Wishart, T.M., Puddifoot, C.A., Alvarez, S., de Lera, A.R., Wyllie, D.J., Compston, D.A., Pedersen, R.A., Gillingwater, T.H., et al. (2011). Retinoid-independent motor neurogenesis from human embryonic stem cells reveals a medial columnar ground state. Nat. Commun. *2*, 214.

Pouya, A., Satarian, L., Kiani, S., Javan, M., and Baharvand, H. (2011). Human induced pluripotent stem cells differentiation into oligodendrocyte progenitors and transplantation in a rat model of optic chiasm demyelination. PLoS One *6*, e27925.

Rice, C.M., Cottrell, D., Wilkins, A., and Scolding, N.J. (2013). Primary progressive multiple sclerosis: progress and challenges. J. Neurol. Neurosurg. Psychiatry *84*, 1100–1106.

Sim, F.J., Zhao, C., Li, W.W., Lakatos, A., and Franklin, R.J. (2002). Expression of the POU-domain transcription factors SCIP/Oct-6 and Brn-2 is associated with Schwann cell but not oligodendrocyte remyelination of the CNS. Mol. Cell. Neurosci. *20*, 669–682.

Sim, F.J., McClain, C.R., Schanz, S.J., Protack, T.L., Windrem, M.S., and Goldman, S.A. (2011). CD140a identifies a population of highly myelinogenic, migration-competent and efficiently engrafting human oligodendrocyte progenitor cells. Nat. Biotechnol. *29*, 934–941.

Song, B., Sun, G., Herszfeld, D., Sylvain, A., Campanale, N.V., Hirst, C.E., Caine, S., Parkington, H.C., Tonta, M.A., Coleman, H.A., et al. (2012). Neural differentiation of patient specific iPS cells as a novel approach to study the pathophysiology of multiple sclerosis. Stem Cell Res. (Amst.) *8*, 259–273.

Stacpoole, S.R.L., Spitzer, S., Bilican, B., Compston, A., Karadottir, R., Chandran, S., and Franklin, R.J.M. (2013). High yields of oligodendrocyte lineage cells from human embryonic stem cells at physiological oxygen tensions for evaluation of translational biology. Stem Cell Rep. *1*, 437–450.

Wang, S., Bates, J., Li, X., Schanz, S., Chandler-Militello, D., Levine, C., Maherali, N., Studer, L., Hochedlinger, K., Windrem, M., and Goldman, S.A. (2013). Human iPSC-derived oligodendrocyte progenitor cells can myelinate and rescue a mouse model of congenital hypomyelination. Cell Stem Cell *12*, 252–264.

Warren, L., Manos, P.D., Ahfeldt, T., Loh, Y.H., Li, H., Lau, F., Ebina, W., Mandal, P.K., Smith, Z.D., Meissner, A., et al. (2010). Highly efficient reprogramming to pluripotency and directed differentiation of human cells with synthetic modified mRNA. Cell Stem Cell *7*, 618–630.

Windrem, M.S., Schanz, S.J., Guo, M., Tian, G.F., Washco, V., Stanwood, N., Rasband, M., Roy, N.S., Nedergaard, M., Havton, L.A., et al. (2008). Neonatal chimerization with human glial progenitor cells can both remyelinate and rescue the otherwise lethally hypomyelinated shiverer mouse. Cell Stem Cell *2*, 553–565.

Yamada, M., Johannesson, B., Sagi, I., Burnett, L.C., Kort, D.H., Prosser, R.W., Paull, D., Nestor, M.W., Freeby, M., Greenberg, E., et al. (2014). Human oocytes reprogram adult somatic nuclei of a type 1 diabetic to diploid pluripotent stem cells. Nature *510*, 533–536. http://dx.doi.org/10.1038/nature13287.